

Evaluation of Torque and Axial Loading Physics for Atmospheric Icing Sensors

Umair N. Mughal and Muhammad S. Virk

Atmospheric Icing Research Team
Narvik University College,
Narvik, Norway
Email: unm@hin.no

Abstract—Measuring icing load and icing rate are important parameters for an atmospheric icing sensor. A new icing sensor has recently been designed and developed at Narvik University College for measuring atmospheric icing rate, icing load and icing type. Unlike the existing atmospheric icing sensors commercially available in market, which uses the axial loading for measuring icing load and icing rate, this new sensory system measures icing load and icing rate using the torque loading physics. The performance of this new icing sensor has been tested and validated at cryospheric environment simulator Japan. This research work focus upon the lab based experimentation and evaluation of axial loading and torque loading sensory physics during an icing event. Results show a significant performance difference between torque and axial loading physics for atmospheric icing sensors.

Keywords—Atmospheric Icing Sensor; Icing Load; Icing Rate; Axial Loading; Torque Loading

I. INTRODUCTION

A. Atmospheric Ice

Atmospheric icing primarily occurs due to the accretion of ice on structures or objects under certain conditions. Generally an icing event is defined as periods of time where the temperature is below $0^{\circ}[C]$ and the relative humidity is above 95%. Ice accretion can be defined as, *any process of ice build up and snow accretion on the surface of objects exposed to the atmosphere* [4]. Liquid below $0^{\circ}[C]$ is called supercooled liquid, which creates atmospheric icing. This accretion can take place either due to freezing precipitation or freezing fog. It is primarily freezing fog that causes this accumulation, which occurs mainly on mountaintops, which is particularly dominant in Norway [1]. It depends mainly on the shape of the object, wind speed, temperature, liquid water content (amount of liquid water in a given volume of air) and droplet size distribution (conventionally known as the median volume diameter). Sometimes ice crystals have a thin coating of water even at temperatures well below freezing, which form clouds. These ice crystals join together to form flakes and reach ground as snow via air passage with temperature less than zero [5]. Snow crystal forms when tiny supercooled cloud droplets (about $10[\mu m]$ in diameter) freeze. However, if the outer coating of water freezes of the combined ice crystals during its path via a air passage with temperature less than zero then they form snow pellets, which are sometimes called as *graupel*. Also, if there is a hot layer of air just below the cold layer of air then they reach ground as *sleet*. Sometimes these small droplets with water coating are not successful in combining with other droplets and they get affected by the surrounding air currents but eventually they fall on the surface, they are called *drizzle*, which is different than *fog* as it doesn't

fall. Drizzle drops are of $0.5[mm]$ but drops larger than this are raindrops. *Hail* is another form of ice. Ice crystals when drop towards the surface they are sometimes passed through very moist air passage due to which they are coated with liquid water, which by strong wind is moved upward where water freezes and then they move down and get covered by liquid water and then moves up to become solid. This process is continued and then it becomes to fall. *Cloud formation* is motivated by a seed or crystalline skeleton on which very tiny, supercooled water droplets can freeze to form snowflakes or soft ice (*graupel*). Naturally, these seeds are random particles of soil, dust, sand, and salt. Artificially they are of two types *glaciogenic* (ice forming e.g., silver iodide or dry ice crystal) or *hygroscopic* (water attracting e.g., small salt particles as potassium chloride) [8].

B. Applications of Atmospheric Icing Sensors

Atmospheric icing is a natural phenomenon, which cannot be avoided in Cold Regions. However, it definitely has some physical loading characteristics on human activities and their associated inventories. On the basis of its loading aspects we can distinguish the effects of atmospheric ice on three classes [8], which are

- a *Static Loads*: Atmospheric ice, particularly (rime and glaze) is when deposited on some static structure, it increases its mechanical weights. Hence it constrains, the design characteristics (particularly factor of safety) of any civil or mechanical structure to be developed in Cold Regions.
- b *Dynamic Loads*: This atmospheric ice, when deposited on the dynamic structures e.g., free dynamic structure as like power cables and motorized dynamic structures as like wind turbines or automobile or ships/boats create additional dynamic loads on these surfaces, which need to be overcome by either anti/de icing techniques in case of free dynamic structures or through increasing the power delivered to such systems.
- c *Wind Action on iced structure*: It is expected that if the structure is iced, its effective geometry will be altered, which in turn reduces the aerodynamic efficiency of structures. This additional drag cannot be completely controlled, however efficient anti/de icing techniques through a good feedback from atmospheric icing sensor may reduce the losses.

Atmospheric ice can be a big problem for different industries working in Cold Regions. The potential affected stakeholders can be [8],

- i *Wind Turbine Industry*: One can improve the efficiency of Wind Turbines by installing an atmospheric icing sensory

network, which should control turbine pitch by providing feedback to filter out the atmospheric icing loading and rate errors

- ii *Oil and Gas Industry due their Onshore and Offshore Installations:* These sensors can be utilized in the big installations of oil and gas platforms in Arctic Region. The output from these sensors can be a good feedback for active monitoring of atmospheric icing activities and its remedies through a good anti/de icing system
- iii *Automobiles Industry:* In Automotive industry these sensors are required to be installed in order to sense the real time atmospheric icing activity on the road surfaces. These sensors can be interconnected with the Road Services via GPS so that accelerated responses for road maintenance can be conducted.
- iv *Power Industry due to the ice on the long power networks:* On power networks, one cannot completely calculate the icing load (which can be very critical). This load if it remains on the power line can be less dangerous than if it suddenly falls its reaction can damage the system. However, active monitoring of icing rate and icing load may reduce this problem if it is connected with some semi active dampers (e.g., magnetorheological damper) mounted on the power cable connections on the pole.

This paper is divided in five sections. In section II, it is aimed to discuss the atmospheric icing load measurement techniques through International Standards/Recommendations and some details about the commercially available atmospheric icing load sensors along with their necessary physics. Section III deals with the torque loading basics and the need to utilize this technique for measuring atmospheric icing load and rate. Section IV starts with an introduction of Cryospheric Environmental Simulator and leads towards performing series of experiments to validate the usefulness of torque loading over axial loading. The concluding section V is divided into smaller parts to comment on various aspects of experimental results.

II. ATMOSPHERIC ICING LOAD MEASUREMENT

To design a new atmospheric icing sensor, in order to measure icing load and icing rate, it is important to understand the existing atmospheric icing rate and icing load sensors. Power requirements for the removal of snow and ice is different hence to distinguish between snow and ice can be considered to be a limiting factor for de-icing system, because most devices for the removal of snow are normally ineffective for the efficient removal of ice or hard packed snow [3]. It is therefore important to distinguish between different types of atmospheric ice. Presently as found, there are commercially available atmospheric icing load sensors, which are only based upon axial loading physics e.g., Ice Load Monitor and Ice Meter [2]. As recommended in international standard ISO 12494 [7], a standard way of measuring ice accretion is to measure the load of atmospheric ice on a steel rod that is 0.5[m] high (1[m] if heavy icing is expected) and has the diameter of 30[mm]. The rod must be freely rotating or *forced to rotate at a constant speed*. When ice accumulates on the steel rod, aerodynamic drag will cause it to rotate in the case of free rotating icing load monitor, always facing the least amount of the iced part towards the wind. This doubling of length of the steel rod due to heavy icing is primarily aimed

to uniform the drag distribution along its profile. By measuring the weight of the iced steel rod with the help of load cells, the amount of ice that has accreted can be determined. Two ice sensors (ice monitor & ice meter) have been developed on the basis of this technique. The following sections describes these two sensors. However, till date none of the atmospheric icing sensor is utilizing torque loading physics, which is also recommended in ISO 12494 [7].

A. The Ice Monitor

The Ice Monitor measures the mass of accumulated ice gravimetrically. The working element is a freely rotating steel pipe resting on a rod placed on a load cell. As ice accumulates on the freely rotating steel pipe, the ice load is weighed by the load cell, see Figure 1. The Ice Monitor is manufactured by SAAB Technologies and was initially developed for power line surveillance systems. It can measure the rate because the readings from the load cell are recorded with time. The Ice-Monitor is not able to detect ice over a wide area and cannot distinguish between the two types of in-cloud icing.



Figure 1. Ice Load Monitor [13]

B. Ice Meter

The ice meter was developed by the Institute of Atmospheric Physics, Prague, Czech Republic. It measures the mass of icing accumulated on the surface of the collector. It has a horizontal rod, which is coupled with a cylindrical collector to the tensometric. The cylinder is orientated vertically in order to eliminate the detection of wet snow as much as possible but the orientation of this cylinder can be changed to horizontal, if required, see Figure 2. In this sensor, the mass of accumulated ice is measured by means of a tensometric bridge (strain gauge load sensor) the output of which is tied to the precise AD converter. The digital signal is preprocessed by a micro-controller, which assigns the time and stores the data into the device memory. In order to prevent the freezing of the horizontal rod, which couples the cylindrical collector to the tensometric, which is located together with the electronics in the housing. The passage through the housing may be heated depending on the passage temperature. A test electromechanical impulse is applied each hour to verify the free force transition to the tensometric, and thus to check whether the acquired data are reliable or not [6].

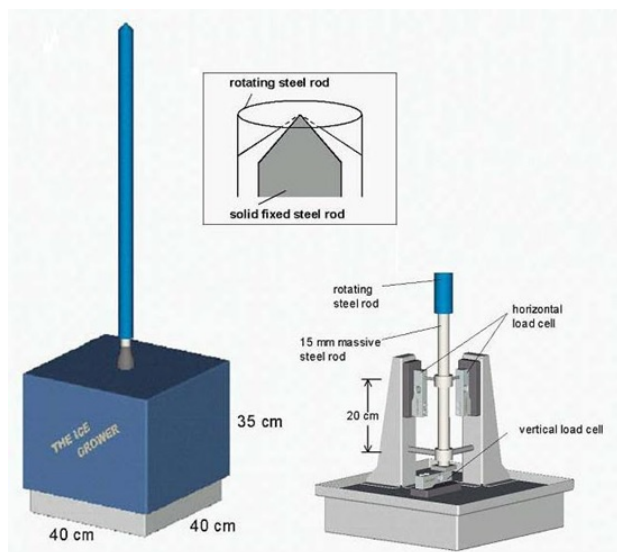


Figure 2. Ice Meter [6]

C. Study of the Physics of Axial Load Based Ice Sensing Methodology

The load is normally described by the way they are applied. If the line of action of the loads is applied parallel to the surface they are called shear loads and when they are applied perpendicular to the surface they are called axial loads, see Figure 3. Although there are many techniques to measure these loads but the most common are associated with piezoelectric sensor and strain gauge sensing elements.

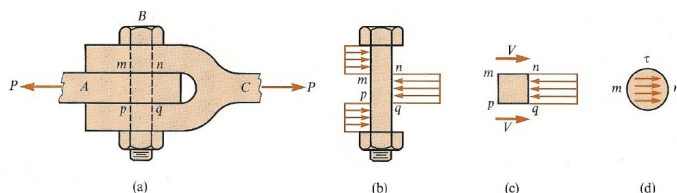


Figure 3. Axial and Shear Load (a). Typical clevis joint, (b). FBD of bolt, (c). FBD of section mnqp, (d). Shear Force on Section mn

D. Piezoelectric Sensing

This sensing technique works by converting the force or strain by converting it into electric charge. Its primary application is in the vibration industry, however it can also be used for load sensing. Piezoelectricity is a property, which is possessed by some materials, which is activated when are acted by some force. Piezoelectric materials have a recoverable strain of 0.1 % under electric field; they can be used as sensors. They may be polymers (e.g., polyvinylidene fluoride *PVDF*) or ceramic materials (e.g., Lead Zirconate Titanate *PZT*). If you apply a static force to a piezoelectric force sensor, then the charge output generated initially will leak away and the output of the sensor will ultimately return to zero. This discharging rate of the charge is exponential and is based on the sensor's discharge time constant, *DTC*. Mathematically the charge characteristics can be described as [9],

$$\begin{aligned} Q_x &= d_{xy} F_y \frac{b}{a} \\ q_x &= Q_x e^{-\frac{t}{RC}} \end{aligned} \quad (1)$$

where Q_x is the amount of charge stored in the piezoelectric material due to the orthogonal force F_y , a and b are the characteristic dimensions of the sensor parallel and orthogonal to the F_y respectively, d_{xy} is the characteristic piezoelectric coefficient (or calibration coefficient of the material), q is the instantaneous charge, R resistance prior to amplified and C is the total capacitance prior to amplifier.

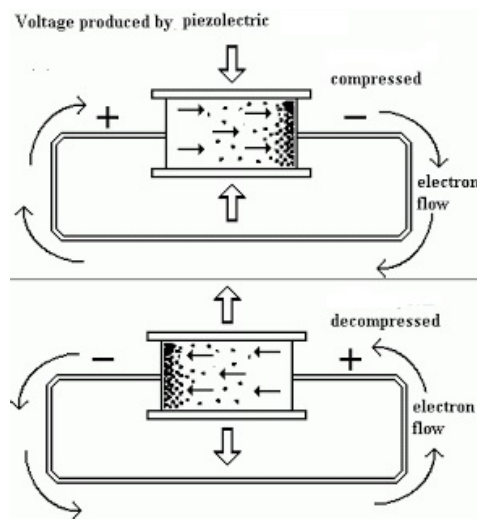


Figure 4. Piezoelectric Sensing [9]

E. Strain Gage Sensors

This technique is more suitable for precise measurement of static loads or a quasi dynamic loads. Within the elastic limits of the material, when a stress is applied to an electric conducting material its electrical conductance R_x changes due to the change in its geometry. This change in conductance is then further measured using a wheatstone bridge (special combination of resistors), which is then further used to measure the load. The resistance change in the wheatstone bridge delivers a voltage, which deliver the strain and hence the force. This special combination of wheatstone bridge is shown in Figure 5b.

$$\begin{aligned} q_x &= Q_x e^{-\frac{t}{RC}} \\ \frac{R_2}{R_1} &= \frac{R_x}{R_3} \\ R_x &= \frac{R_2}{R_1} R_3 \\ V_G &= \left(\frac{R_x}{R_3 + R_x} - \frac{R_2}{R_1 + R_2} \right) V_s \end{aligned} \quad (2)$$

This concept has been utilized in the Ice Load Monitor Sensor by SAAB Technologies, see Sec. II-A.

F. Problems with existing Ice Load and Icing Rate Measurement Systems

1) *Measurements in Czech Republic [7]*: The icemeter has been operated on the Milesovka peak from 2000. Although icemeters installed in the site measured correctly most of the time, but there were also some time periods when the instruments gave obviously wrong negative values. These times

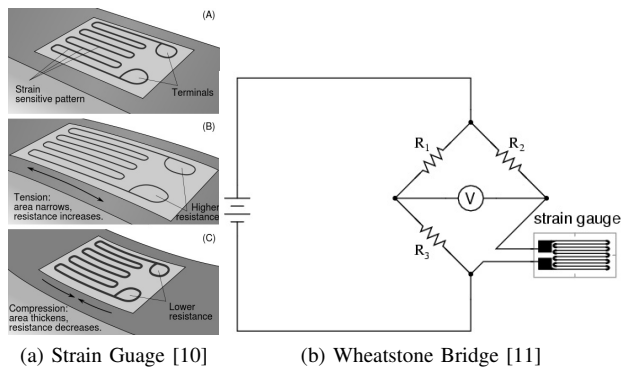


Figure 5. Strain Gauge Sensing

can usually be associated with the periods when the horizontal rod coupling the tensometric with the vertical collector became icebound to the instrument housing. Thus there was no free force transition, which can be identified by not observing a proper electromechanical pulse in the data. The following changes are expected to be made in icemeter for its better performance,

- i Possibility to build an instrument with a rotating collector.
- ii More focus on the sensors that measure accumulated icing.

III. TORQUE MEASUREMENTS

An analytical expression between mass moment of inertia and the supplied current (3) was developed (for more see Mughal et. al. [14]),

$$J = aI_{in} - b \quad (3)$$

where $a = \alpha V_{in} / \beta \gamma \omega_m^3$ and $b = \eta / \beta \gamma \omega_m^3$ will be constant. The (3) relation was further modified to take the form (4) in order to compare the results of this new sensor with a standard ice load sensor.

$$\delta m_{ice} = A \delta I_{in(ice)} + B \quad (4)$$

Where $A = \frac{a}{R_{ice}^2}$ and $B = \frac{aI_{in} - J - b}{R_{ice}^2}$. The (4) relation is named as *MuVi Current-Mass ($\delta I - \delta m$) Relation*.

A. Requirement of Torque Loading

As it is understood from [7] that presently there is no atmospheric icing sensor in the commercial market that can measure the icing load, which is uniformly distributed along the sensory surface. All the commercially available sensors (e.g., Ice Load Monitor), measure the non uniform loading on a freely rotating surface, however it is recommended in [7] that a rotary sensory system will be more suitable. A new sensor have been developed by the authors to measure icing load and icing rate. This sensor is based upon the rotary dynamics where the collector rotates at a constant speed in order to allow ice to uniformly distribute around the rotary collector.

IV. CRYOSPHERIC ENVIRONMENT SIMULATOR CES, SHINJO JAPAN

Cryospheric Environmental Simulator is an experimentation facility of NIED at Shinjo, Japan. They provide the capacity to perform basic and applied studies related with snow and ice disasters using a snow fall machine and icing wind tunnel. For this experimentation to evaluate the performance of this new sensor, Cryospheric Environmental Simulator CES was the most suitable choice, which had the facility to test this sensor both in Icing Wind Tunnel and Snow Simulator. The facilities and specifications of CES are provided in Table I, which are taken from [12],

TABLE I. FACILITIES AND CONTROLLABLE PARAMETERS IN COLD ROOM AT CES, NIED JAPAN

Facilities	Specifications		
	Variables	Limitations	Comments
General Conditions in the Cold Room	Temperature	$-30^\circ \rightarrow +25^\circ$	—
Snowfall Machine A	Snowfall Intensity	0 —	water equivalent
	Crystal Type	Dendrites	$0.5 \rightarrow 5[mm]$
	Area	$3 \times 5[m]$	—
Snowfall Machine B	Snowfall Intensity	0 —	water equivalent
	Crystal Type	Sphere	Diameter $0.025[mm]$
	Area	$3 \times 5[m]$	—
Rainfall Machine	Rainfall Intensity	0 —	—
	Area	$3 \times 5[m]$	—
Solar Simulator	Solar Radiation	0 —	—
	Area	$3 \times 5[m]$	—
Experiment Table	Size	$3 \times 5[m]$	—
	Inclination	$0 \rightarrow 45^\circ$	—
Wind Tunnel	Wind Speed	0 \rightarrow $10[m/s]$	—

A. Calibration of Ice Load Monitor and new atmospheric Icing Sensor

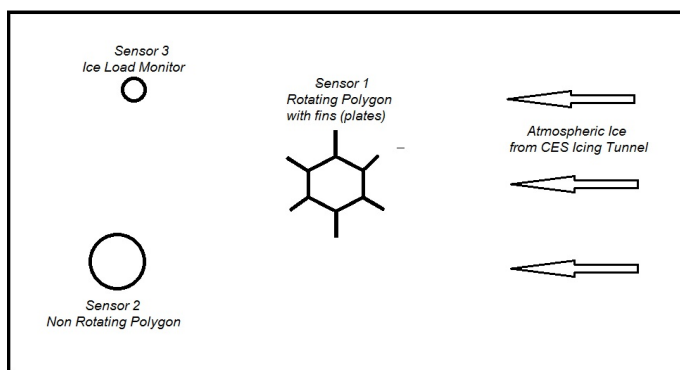
1) *Ice Load Monitor*: It is found that this standard sensor have never been tested in any standard icing tunnel or snow simulator as like Cryospheric Environmental Simulator and if it is tested then it is not published/reported (the details of CES Simulator will be discussed in Sec IV). The Ice Load Monitor deliver a current output as a measure of icing load. This sensor was calibrated at Narvik University College and the calibration equation is given by (5). For more details on this calibration, see Mughal and Virk [15].

$$I = 0.0017 \delta \delta m_{ILM_{cal}} + 4.435 \quad (5)$$

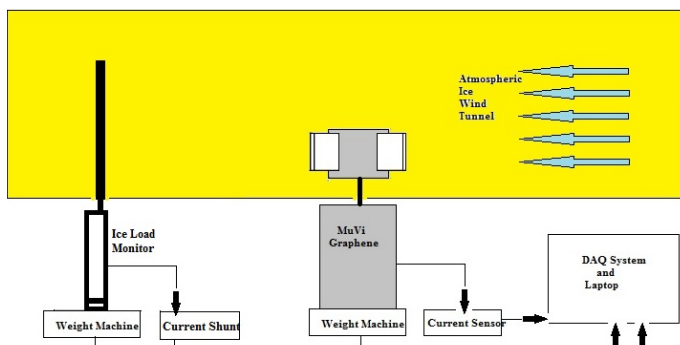
2) *New Atmospheric Icing Sensor*: This was calibrated using standard rotary masses on the sensor shaft and measuring the output current as a measure of mass moment of inertia. The electronic setup for calibration can be seen in Figure 6c. The calibration equations thus obtained is given by (6) (for more details on this, see Mughal et. al. [14]),

$$I = 2.91 \times 10^{-7} J_{MuVi_{cal}} + 328.64 \quad (6)$$

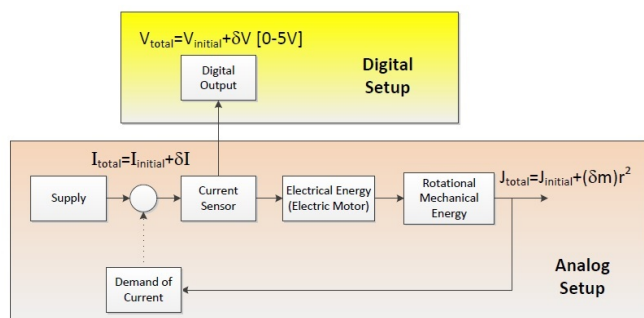
Where J is in $[gm\ mm^2]$ and $I_{measured}$ is in $[mA]$.



(a) Experimental Table - Top View



(b) Experimental Table - Side View



(c) Electronic Setup

Figure 6. Experimental and Electronic Setup, CES Japan [15]

B. Experiment performed at CES, Japan

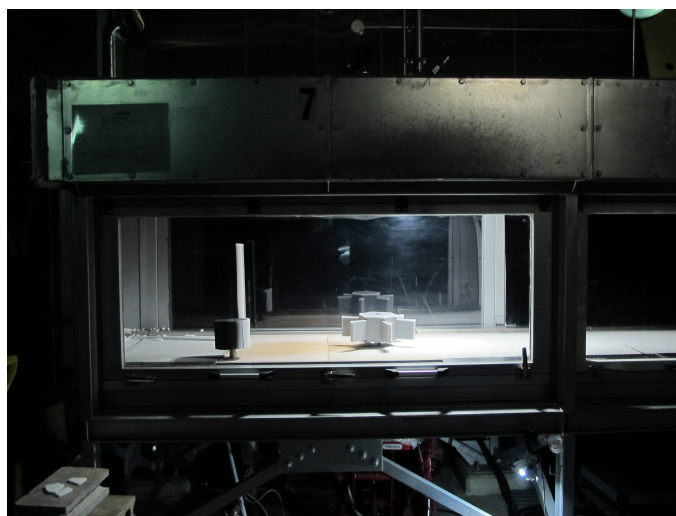
The experiment was performed in Icing Wind Tunnel using three different sensors, arranged on the sensory table as can be seen in Figure 7a where Sensor 1 is the rotary sensor with complete electronics of this new sensor, Sensor 2 is the additional sensor, which is just a geometric shape to understand the deposition of atmospheric ice in order to optimize the non rotary parts parts of new sensor. The experimental conditions during the experiment can be seen in Table II, which is followed by Figure 7b reflecting the measurement setup under the experimental table. The graphical results of this experiment are shown in Figure 8 [8].

TABLE II. EXPERIMENTAL CONDITIONS FOR EXPERIMENT 1

Before Experiment	
Condition/Variables	Specifications
Date of Experiment	17/02/2014
Experiment Number	1
Experimental Facility	CES Icing Wind Tunnel
Sensor 1	Rotating hexagon with plates
Sensor 2	Non rotating cylinder
Sensor 3	Freely rotating Ice Load Monitor
Tunnel Temperature	-15°
Time of Experiment	170[<i>min</i>]
Wind Speed for first 60[<i>min</i>]	6[<i>m/s</i>]
Wind Speed for next 110[<i>min</i>]	10[<i>m/s</i>]
Mass of Sensor 1 (without ice)	8936[<i>gm</i>]
Mass of Sensor 2 (without ice)	591[<i>gm</i>]
Mass of Sensor 3 (without ice)	0[<i>gm</i>]
After Experiment	
Mass of Sensor 1	9735[<i>gm</i>]
Mass of Sensor 2	866[<i>gm</i>]
Mass of Sensor 3	480[<i>gm</i>]



(a) Sensors Arrangement in Icing Tunnel - Front View



(b) Sensors Arrangement in Icing Tunnel - Side View

Figure 7. Experimental Setup in Icing Tunnel

The icing rate on this new sensor can be determined using the relation (7) whereas the icing rate on Ice Load Monitor can be determined using the relation (8). The associated curves for these equation are shown in Figure 8a, which clearly reflect that this new sensor, have more capability of holding uniform distribution of atmospheric ice then a freely rotating Ice Load Monitor. Also, the manufacturers of Ice Load Monitor claim that after 40[gm] their sensor will be able to predict icing load and icing rate and as found by experiments this 40[gm] on ice load monitor is collected in around 30[*min*] whereas the same 40[gm] of mass on new sensor is collected in first 5[*min*] and that too uniformly. This uniform distribution is very important for additional mass moment of inertia on the sensor to deliver additional current as a measurable quantity. The calibrated relation between mass moment of inertia and current loading is given by (6) whereas the experimental mass moment of inertia and current loading equation is given as (9) and graphical results are shown in Figure 8b. The experimental section was bounded by walls (in icing wind tunnel), and it may be one of the possible reason of deviation between calibrated and experimental $I - J$ Relation but nevertheless this can be adjusted through proper calibration. The additional mass and additional current calibrated equation of Ice Load Monitor is given by (5) and the experimental relation is given by (10) and the results are shown in Figure 8c. These results of Ice Load Monitor shows that for a mass range of 0 → 500[gm] the current variation is around 4.5 → 5.3[*mA*] ideally and 5 → 6.8[*mA*] experimentally, which have more potential of noise interference. The mass current relation of this new sensor was also determined experimentally and is given by (11) and the graphical representation can be seen in Figure 8d. This equation of this new sensor was then compared with the (10), which clearly reflect that this new sensor for a mass domain of 40 → 800[gm] was having a current range of 0 → 150[*mA*], which is quite reasonable to filter noise and other calibration errors. The R^2 value reflect that linear relations of experimental of this new sensor are 96% whereas for Ice Load Monitor this value is 88% linear.

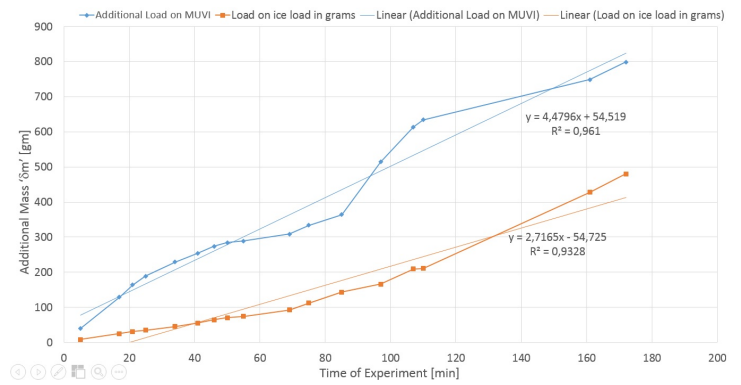
$$\delta m_{MuVi} = 4.480t + 54.519 \tag{7}$$

$$\delta m_{ILM} = 2.716t - 54.725 \tag{8}$$

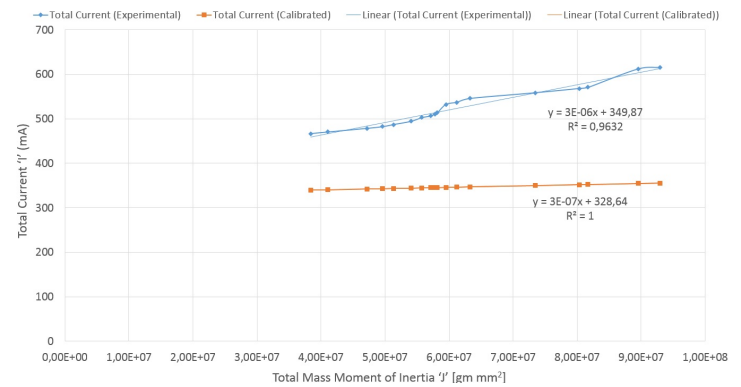
$$I = 2.84 \times 10^{-6} J_{MuVi_{exp}} + 349.87 \tag{9}$$

$$\delta I = 0.0031\delta m_{ILM} + 5.259 \tag{10}$$

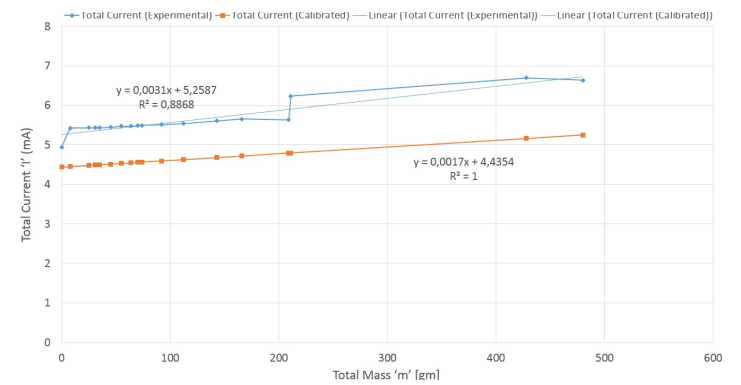
$$\delta I = 0.1936\delta m_{newsensor} - 7.21 \tag{11}$$



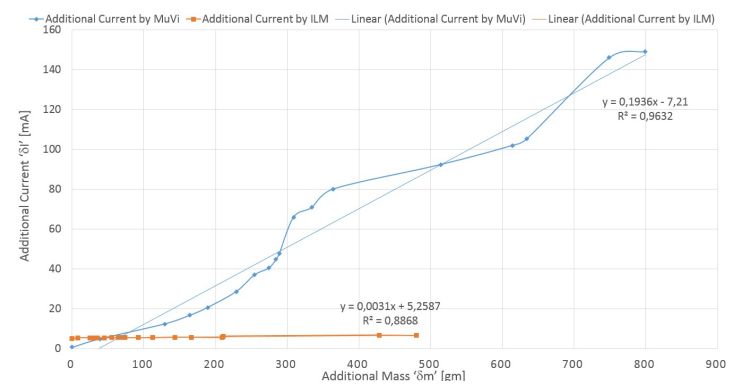
(a) Atmospheric Ice Growth Rate (Mass-Time Curve)



(b) Current Mass Moment of Inertia Curve (I-J Curve) of New Sensor at 6rpm



(c) Current Mass (I-m Curve) of Ice Load Monitor



(d) Additional Current Additional Mass ($\delta I - \delta m$ Curve)

Figure 8. Graphical Results of Experiment 1 in Icing Wind Tunnel [15]

V. CONCLUDING DISCUSSIONS

1) *RPM Fluctuations*: The rotational speed of this sensor was selected to be 6rpm. It is found that if the rpm was 5 there were current fluctuations in the range of mA during rotation without any change in load. Also, during experiment it was found that if the rpm was increased to 8 chances of non uniform deposition of ice on the sensor, which may lead to additional errors.

2) *Sensitivity*: The results of experiment clearly reflect that new sensor provide sufficient deposition of atmospheric ice ice at an optimized rpm of 6. Also, the current range to measure icing load and icing rate is quite reasonable to determine the required parameters. This new sensor is more sensitive than Ice Load Monitor because if it is said that 40[gm] of mass for Ice Load Monitor as the starting mass for new sensor than it is collected within first 5 → 10[*min*] on new sensory unit and it is more than 30[*min*] for Ice Load Monitor. The reason of this mass deposition is due to the rotary physics associated with new sensor and the surface area of Ice Load Monitor is around $50 \times 10^3[mm^2]$ and new sensor is around $112 \times 10^3[mm^2]$.

3) *Saturation*: The saturation limit for the motor was adjusted to be around 1[A]. If the demand in current from the rotary unit of new sensor exceeds 1[A] than the motor would stop. The maximum mass for new sensor was tested for a mass of 800[gm] for a time period of 170[*min*] and it is found that new unit have still more potential to hold the ice mass.

4) *Performance*: The sensor have been tested in the Cryospheric Environmental Icing Simulator at a temperature of $-15^\circ[C]$ and have performed satisfactory without any error signal. This sensor have not been tested in the field, however it is aimed to test this sensor in the field in the upcoming Winter 2014 – 15. The calibration error may have been associated with the poor performance of the sensor, however this have been true if the results of experiment were not linear. The experimental results show that the new sensor have a good performance potential than Ice Load Monitor, however Ice Load Monitor is already in use by industry in the field whereas new sensor still has not yet been commercialized.

5) *Error Diagram*: The error diagrams from experiment 1 to experiment 4 reflect that new sensor have very low error in the start but it increases linearly due to the deviation between the experimental slope and calibrated slope of new sensor but nevertheless it can be improved by adopting proper calibration. The error is calculated using the following (12),

$$\%Error = \left| \frac{I_{exp} - I_{cal}}{I_{cal}} \right| \times 100. \quad (12)$$

The error diagram of Experiment between new sensor and Ice Load Monitor as calculated by (12) is shown in Figure 9. The error results shows that the % error range of new sensor is starts from 0% and increases linearly because experimental slope of J-I Relation of new sensor (9) is one order higher than the calibrated slope of (6). The error on Ice Load Monitor is around 10 – 30%. These all results reflect new sensor as a good solution for measuring Icing and Snow Load Rate if properly calibrated as it has more potential to deposit ice and give reasonable reading count, which is required to filter the cold climate current errors.

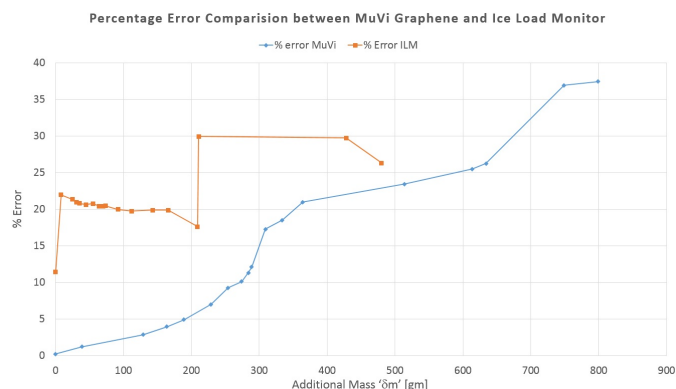


Figure 9. Experiment 1 Percentage Error Diagram

ACKNOWLEDGMENT

We acknowledge the research funding from Research Council of Norway, project no. 195153/160 and partially by the consortium of the ColdTech RT3 project - Sustainable Cold Climate Technology.

REFERENCES

- [1] M. C. Homola, "Atmospheric Icing on Wind Turbines", Doctoral Theses at NTNU 2011:259, 2011.
- [2] U. N. Mughal and M. S. Virk, "Atmospheric icing sensors - An insight", The Seventh International Conference on Sensor Technologies and Applications, ISBN 978-161208-296-7, August 25-31, 2013, pp. 191-199.
- [3] C. D. Kuhumonen, "Ice removing machine", U.S. Patent 4186967, 1980.
- [4] H. F. Foder, "ISO 12494 - Atmospheric icing on structures and how to use it", ISO 12494:2001, ISBN 1-880653-51-6, June 2001.
- [5] S. W. Trimble, "Encyclopedia of Water Science - 2nd Edition", CRC Press, ISBN 978-0-8493-0-9627-4, 2008.
- [6] <http://www.ufa.cas.cz/html/upperatm/chum/namraza/1cingmeasczech2.pdf>, Last Access date: September 10, 2014.
- [7] S. Fikke, "Cost 727 - Atmospheric icing on structures; measurement and data collection on icing", ISSN 1422-1381, MeteoSwiss, 2007.
- [8] U. N. Mughal, "Design and Development of Robust Atmospheric Icing Sensor", PhD Thesis submitted at the Department of Physics, University of Oslo, July 2014.
- [9] <http://migyanesfertechno.blogspot.no/2012/01/piezoelectricidad.html>, Last Access date: September 10, 2014.
- [10] http://en.wikipedia.org/wiki/Strain_gauge, Last Access date: September 10, 2014.
- [11] http://www.allaboutcircuits.com/vol_1/chpt_9/7.html, Last Access date: September 10, 2014.
- [12] http://www.bosai.go.jp/seppyo/jikkentou/jikkentou_syokai_e.html, Last Access date: September 10, 2014.
- [13] http://www.combitech.com/Documents/IceMonitor_Produnktblad_Combitech.pdf, Last Access date: September 10, 2014.
- [14] U. N. Mughal, M. S. Virk, K. Kosugi, and S. Mochizuki, "Experimental Validation of Icing Load Using Rotary Physics", Manuscript submitted in International Journal of Cold Regions Science and Technology, August 2014.
- [15] U. N. Mughal and M. S. Virk, "Performance Evaluation of MuVi-Graphene and Ice Load Monitor in icing conditions", Manuscript submitted in International Journal of Cold Regions Science and Technology, August 2014.